Retrieving the complex polarizability of single plasmonic nanoresonators

M. Celebrano,[1,*] M. Savoini,[1] P. Biagioni,[1] M. Zavelani-Rossi,[1] P.-M. Adam,[2] L. Duò,[1] G. Cerullo,[1] and M. Finazzi[1]
[1]*Dipartimento di Fisica, Politecnico di Milano, Piazza Leonardo da Vinci 32, 20133 Milano, Italy*
[2]*Laboratoire de Nanotechnologie et d'Instrumentation Optique, Université de Technologie de Troyes, 12 Rue Marie Curie, 10010 Troyes, France*
(Received 29 April 2009; revised manuscript received 4 September 2009; published 6 October 2009)

The complex optical polarizability of a nano-oscillator determines the way it couples to light and to other nano-objects in its environment. Hence, its experimental evaluation at the single-particle level represents a crucial task in nano-optics. In this work we demonstrate that both phase and amplitude of a nanoresonator polarizability, which are embedded in its near-field response, can be decoupled by combining near-field and confocal far-field extinction imagings. The interpretation of our measurements based on a simple analytical model is further confirmed by finite-difference time-domain calculations.

DOI: 10.1103/PhysRevB.80.153407 PACS number(s): 73.22.Lp, 42.30.Rx, 68.37.Uv, 78.67.−n

Introduction. Noble-metal nanoparticles have been the subject of an impressive amount of experimental studies over the last decade because of the broad variety of their applications in nano-optics. Their appeal lies in the occurrence of localized surface plasmon (LSP) resonances at visible and near-infrared frequencies, which significantly influence the particle polarizability and produce large local-field enhancement (up to several orders of magnitude) and confinement (on the nanometer scale). It has been shown that noble-metal nanoparticles can be employed as nanoresonators for visible-light enhancement[1–6] and that, in array structures, they can efficiently transport and guide light below the diffraction limit,[7,8] demonstrating the possibility of creating LSP-based networks for light manipulation at the nanoscale.[9] To achieve the best design for such complex systems both analytical modeling[10] and experimental far-field studies[11] have been carried out.

Generally, the optical properties of an ellipsoidal nanoparticle can be described within the framework of the generalized Mie theory or, for more complicated structures, by means of numerical simulations. In practice, plasmonic nanoresonators are greatly affected by the particle morphology: small imperfections can induce shifts in the resonance frequency and affect the resonator quality factor.[12] For this reason, ensemble measurements on metal nanoparticles suffer from inhomogeneous broadening. The ideal solution for characterizing the optical performances of nano-oscillators would thus be addressing single nanoparticles. In this respect, the ability of retrieving the phase response of an individual nano-oscillator is of fundamental importance in novel applications based on coherent control of phase and polarization to guide light via nanoparticle arrays.[13–15] In particular, light propagation in such plasmonic networks is effectively determined by the optical phase response of each single element, which influences the phase relation between different components of the propagating electromagnetic wave and rules the interference phenomena that lead to efficient propagation.

A number of works in the literature have reported single-particle extinction or scattering measurements addressing the LSP spectral behavior by either far-field confocal optical microscopy[16–18] or scanning near-field optical microscopy (SNOM).[19–23] Scattering and extinction cross sections in far-field experiments can be directly related to the absolute value and imaginary part of the particle polarizability,[24] respectively. Stoller *et al.*[18] developed a method to experimentally address the complex polarizability of single gold nanoparticles by combining coherent white-light illumination and differential interference contrast far-field microscopy. Another far-field method to retrieve phase information from a nano-object has been theoretically proposed by Hwang *et al.*[25] and recently applied to nanocrystal quantum dots.[26]

It is now established that near-field extinction spectra bear a strong signature from the phase of the particle polarizability as a result of interference between the radiation from the tip and that from the plasmon excited by the near-field component of the incoming light.[20] However, the particle near-field response is a function of both the phase and the amplitude of the LSP oscillation, hence an additional measurement would be required in order to experimentally separate the two contributions. Moreover, near-field experiments are influenced by the complex spectral dependence of the propagating and evanescent light components in proximity of the aperture and can be affected by the probe-particle coupling, which might results in a shift of the particle resonance frequency. For these reasons, near-field techniques have not been applied so far to the task of experimentally reconstructing the complex polarizability of single metal nanoparticles.

In this work, we show that the combination of far-field and near-field imagings can be effectively exploited to extract the phase response of an optical nano-oscillator and therefore to determine both the phase and the amplitude of its complex optical response. In particular, this method is demonstrated by applying extinction imaging to single gold nanorods.

Experimental. In order to determine the particle complex polarizability, both the near- and far-field responses need to be evaluated in on- and off-resonant conditions. This can be achieved by (i) measuring the response of a particle at different wavelengths or (ii) considering particles with different size at a fixed excitation wavelength. In the following we will apply the second solution on an ensemble of length-varying nanorods in order to disregard the frequency-dependent near-field response of the probe. This allows interpreting the results within a much simpler and reliable analytical model.

The investigated sample consists of an array of Au nanorods fabricated by electron-beam lithography on a fused

silica substrate coated with 95-nm-thick indium tin oxide.[27] The nanorod major axis length l ranges from 80 to 240 nm in steps of 10 nm, while the cross section is rectangular (height $\approx$20 nm; width $\approx$50 nm) with smoothed edges. The interparticle spacing is 2 μm. When illuminated with linearly polarized light parallel to the major axis, the particles display an l-dependent first-order longitudinal LSP resonance in the 500–1500 nm wavelength range[27,28] associated to a dipole charge distribution. In such configuration, the particle electric behavior can be described by a complex polarizability tensor.

Near-field and far-field optical extinction images are collected with a commercial microscope that combines a SNOM system and a transmission confocal scanning microscope (AlphaSNOM, WITec GmbH). Monochromatic illumination is provided by a cw laser diode at 840 nm. For far-field imaging, the sample is illuminated by a 0.8 numerical aperture (NA) objective, while transmitted light is collected in a confocal geometry by a 0.75 NA objective. The collected light intensity is measured by a Si photodiode through a 25 μm pin-hole for background rejection. Single-particle far-field extinction maps are collected while the sample is raster scanned between the objectives. Near-field imaging is performed with a hollow-pyramid SNOM probe (aperture diameter $\approx$100 nm), which is placed in the focus of the illumination objective by a mechanical piezoelectric actuator. This ensures that the whole optical system is left unchanged between far-field and near-field analyses except for the presence of the tip. The polarization state of the light is linear and parallel to the nanorod major axis for both far- and near-field[29] imagings. Probe-sample distance is stabilized by a "soft" tapping mode with low oscillation amplitude ($\approx$2 nm, close to the so-called "noncontact regime").[30] In this regime the tip-particle interaction is strongly reduced. As shown below, this results in a negligible spectral shift of the nanorod LSP resonances.[31]

As a comparison with the experimental results, we have also performed finite-difference time-domain (FDTD) simulations,[32] considering a single nanorod illuminated by a focused Gaussian beam (NA=0.8). The net Poynting vector flux is calculated in transmission geometry, collected with NA=0.75 in order to fully adhere to the far-field experimental setup. The geometry of the simulated nanorods is defined according to their dimensions, with smoothed apexes to better reproduce the shape observed in scanning electron microscopy (SEM) images.

Results and discussion. Near-field extinction maps of the gold nanorods are reported in Fig. 1. Panels (a)–(g) show rods with l ranging from 90 to 150 nm. Line profiles extracted from the images [Fig. 1(h)] allow us to calculate a near-field contrast factor for each nanoparticle defined as

$$C_{\mathrm{nf}} = \frac{I_{\mathrm{nf}} - I_{0,\mathrm{nf}}}{I_{0,\mathrm{nf}}}, \tag{1}$$

where I_{nf} is the light intensity measured when the collection objective and the tip are axially centered on the particle, while $I_{0,\mathrm{nf}}$ is the background, i.e., the transmitted intensity through the tip and the glass substrate away from any particle. The contrast C_{nf} as a function of the particle length is

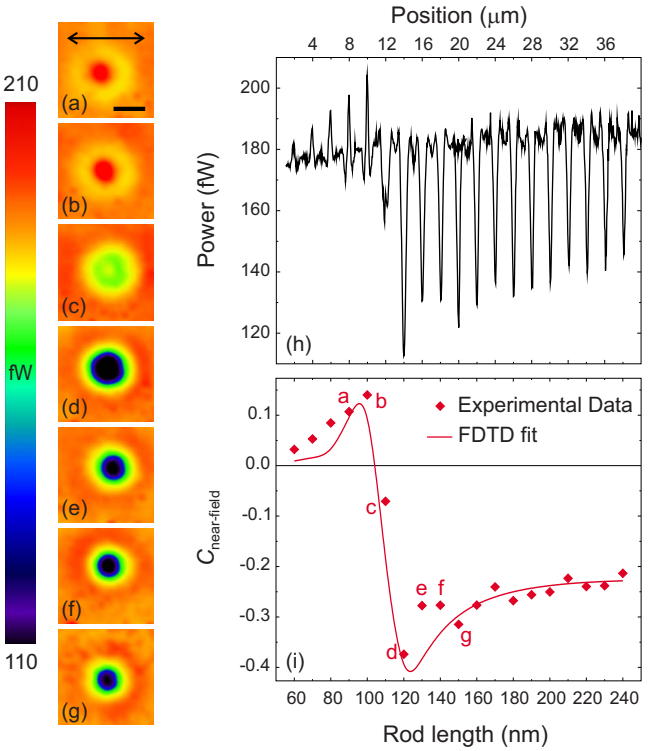

FIG. 1. (Color online) [(a)–(g)] Near-field extinction images of gold nanorods [rod lengths (a) 90, (b) 100, (c) 110, (d) 120, (e) 130, (f) 140, and (g) 150 nm]. The arrow in panel (a) indicates the incident light polarization. Scale bar is 300 nm. (h) Line profile extracted from the near-field extinction map of the nanorod array. (i) Near-field contrast (diamonds). Error bars evaluated from the noise in the images are within the width of the symbols. The solid line represents the fit obtained through FDTD calculation (see text for details). The letters refer to the near-field maps on the left.

shown in Fig. 1(i) (diamonds), from which it can be clearly seen that $C_{\mathrm{nf}}>0$ ($C_{\mathrm{nf}}<0$) for $l<110$ nm ($l>110$ nm), meaning that short (long) nanorods appear brighter (dimmer) than the substrate. A similar optical response has already been reported in the literature to explain the results of an experiment complementary to ours, in which the near-field extinction spectrum of a single particle was collected after broadband excitation. Such a behavior can be interpreted by recalling that the signal measured by the detector is the result of interference between the light emitted by the tip apex and the light scattered by the particle.[20,33] These two contributions can also be thought, in the far field, as generated by two oscillating dipoles: $\mathbf{p}$ located at the tip apex[34] and $\mathbf{p}_{\mathrm{rod}}$ associated with the plasmon oscillation induced on the nanorod by a driving field $\mathbf{E}$ describing the excitation due to the tip near field. The radiant intensity in a given direction can thus be expressed through the superposition of these two dipoles:

$$\frac{dI_{\mathrm{nf}}}{d\Omega} \propto |\mathbf{p} + \mathbf{p}_{\mathrm{rod}}|^2 \approx p^2 + 2\sum_{i,j} p_i^* E_j \,\mathrm{Re}(\alpha_{i,j}), \tag{2}$$

where α_{ij} represents the nanorod polarizability tensor and Ω is the solid angle. In Eq. (2) we have neglected the second-order terms in $\mathbf{E}$ since the light scattered by the rod repre-

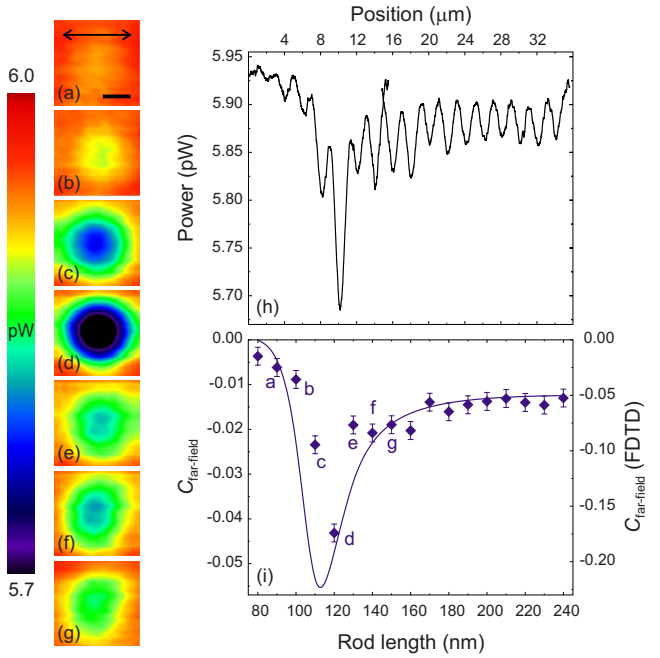

FIG. 2. (Color online) [(a)–(g)] Far-field extinction images of gold nanorods (same as Fig. 1). The arrow in panel (a) indicates the incident light polarization. Scale bar is 600 nm. (h) Line profile extracted from the far-field extinction map of the nanorod array. (i) Far-field contrast (diamonds). Error bars are evaluated from the noise in the images. The solid line represents the FDTD calculation (see text for details)

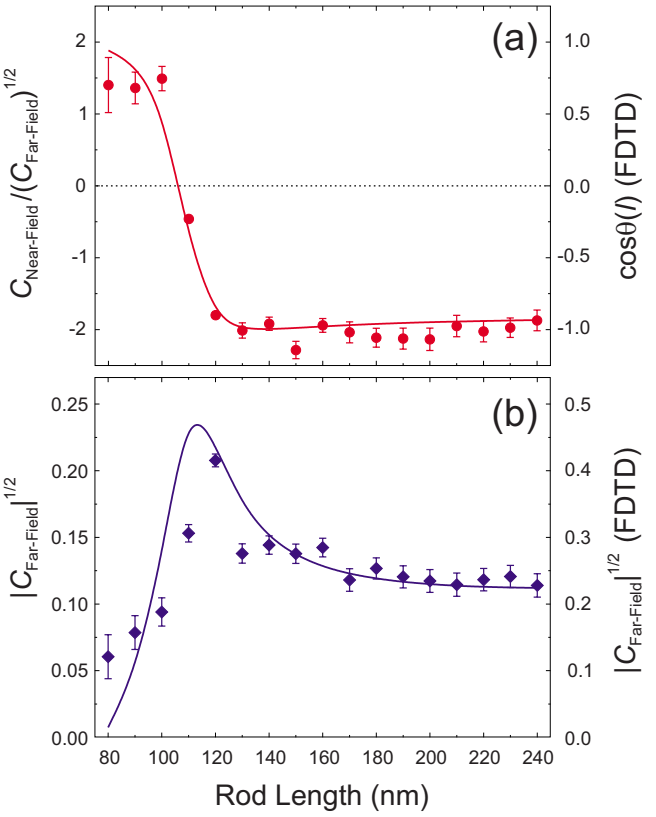

FIG. 3. (Color online) (a) Normalized near-field contrast proportional to $\cos(l)$: experimental data (circles) and fit by simulations (solid line). (b) Square root of the far-field contrast proportional to $A(l)$: experimental data (diamonds) and fit by simulations (solid line). Error bars are derived from those in Figs. 1 and 2.

sents a small contribution to the total radiation propagating to the detector as demonstrated by the relatively low contrast value observed in the near-field images ($|C_{\mathrm{nf}}|<1$). With our experimental geometry we only excite the longitudinal LSP eigenmode and thus probe only one component of α_{ij}, namely, the longitudinal polarizability $\alpha_{\mathrm{lon}}(l)=A(l)e^{i\theta(l)}$. We note that different components of the polarizability tensor can be addressed by changing the near-field polarization state and the collection geometry (e.g., by inserting a polarizer on detection).

The background radiant intensity in the experiments (no particle below the tip) can be written as

$$\frac{dI_{0,\mathrm{nf}}}{d\Omega} \propto p^2. \tag{3}$$

By integrating Eqs. (2) and (3) over the collection solid angle and by recalling that $\mathbf{p} \propto \mathbf{E}$, the measured near-field contrast can be evaluated as

$$C_{\mathrm{nf}} \propto A(l)\cos\,\theta(l). \tag{4}$$

Equation (4) shows that near-field extinction is sensitive to both the amplitude $A(l)$ and the phase $\theta(l)$ of the particle longitudinal polarizability. The proportionality factor depends on the geometry of the experimental setup.[31]

In order to decouple $A(l)$ from $\theta(l)$ in Eq. (4) and get experimental access to each term, we take advantage of the possibility to acquire confocal images with the same system on the same sample. In general, far-field extinction bears signature of both scattering and absorption of the nano-object.[16,24] However, for relatively large gold nanoparticles ($l>30$ nm), the extinction is determined almost completely by scattering, while absorption can be neglected.[16,35,36] The far-field contrast is hence proportional to the square of the absolute value of the particle polarizability:[24]

$$C_{\mathrm{ff}} = \frac{I_{\mathrm{ff}} - I_{0,\mathrm{ff}}}{I_{0,\mathrm{ff}}} \propto A(l)^2. \tag{5}$$

Panels (a)–(g) in Fig. 2 show the far-field extinction maps of the same nanorods as in Figs. 1(a)–1(g). From the line profile shown in Fig. 2(h) we extract $C_{\mathrm{ff}}(l)$, which is shown in Fig. 2(i) (diamonds) together with the value obtained by the FDTD calculations (full line). The simulated C_{ff} value is found to be considerably larger (about a factor of 4) than the measured one. The reduced absolute value for the experimental contrast, compared to the simulated one, has to be attributed to the nonideal experimental background. Apart for this scaling factor, the signature of the LSP resonance in C_{ff} is well reproduced by the simulations. Discrepancies between the calculated and the experimental C_{ff} behavior are due to deviations of the particle size with respect to the nominal values (about $\pm 10\%$) or to the particle fine structure. This is also confirmed by SEM imaging (not shown)

and demonstrates the importance of single-particle characterization.

Note that the resonance condition is fulfilled for particles which show a zero value in the C_{nf} plot[20,33] and a minimum in the C_{ff} one. Incidentally, this behavior can be exploited to evaluate possible probe-particle coupling effects. By inspection of Figs. 1(i) and 2(i) one can realize that the shift between the near-field resonance (zero-crossing point) and the far-field one (minimum) is kept below the discrete length increment in our set of particles (10 nm).

According to Eq. (5), we can now evaluate the pure amplitude response of the plasmon resonance, which can be combined with near-field data to obtain the oscillator phase and completely characterize the particle optical polarizability. In practice, this can be achieved through the normalization of C_{nf} [Eq. (4)] by the square root of C_{ff} [Eq. (5)]. In this way the phase of the LSP oscillation associated with each nanorod is given by the following relation:

$$\cos\,\theta(l) \propto C_{nf}(l)/|C_{ff}(l)|^{1/2}, \tag{6}$$

where the proportionality factor depends on the working conditions. The $C_{nf}/|C_{ff}|^{1/2}$ value obtained from our set of data is shown in Fig. 3(a) (dots) and displays an abrupt variation around the resonance length as expected from the theory of the harmonic oscillator. The proportionality factor in Eq. (6) can be evaluated by considering a nanoparticle with a well-defined phase as a reference. This is the case for off-resonance particles, where the phase of the nano-oscillator is equal to either 0 ($C_{nf}>0$) or π ($C_{nf}<0$). The dependence of $C_{nf}/|C_{ff}|^{1/2}$ on the particle length l is in excellent agreement with the nanorod phase response from the FDTD simulations [solid line in Fig. 3(a)], obtained by evaluating the phase of the re-emitted field close to each particle.

The amplitude $A(l)$ of the polarizability is proportional to the square root of the far-field contrast, which is plotted in Fig. 3(b) for comparison with the phase. Note that the amplitude is not symmetric with respect to the resonance length. This feature reflects the size-dependent radiative damping and depolarization effects in the particle polarizability[37] and the possible presence of a tail due to quadrupolar resonances.[28,38]

Finally, to further support these experimental results and their interpretation, we have combined the simulated l-dependent values of the phase [Fig. 3(a)] and the square root of the far-field extinction computed by FDTD calculations [Fig. 2(i)] in order to fit the near-field contrast C_{nf} according to Eq. (4). The result, displayed in Fig. 1(i) (solid line), shows a very good agreement with the experimental data and highlights the reliability of the near-field approach.

Conclusions. In conclusion, the complex polarizability of gold nanorods has been experimentally obtained by performing combined single-particle near- and far-field extinction measurements. We have shown how the phase of individual nano-oscillators can be extracted from their near-field response (which is determined by both the amplitude and phase of the dipole oscillator) when the far-field extinction (containing mainly information about the oscillation amplitude) is also measured. The phase and amplitude can thus be obtained with the only exception of scaling factors depending on the geometry and detection efficiency of the optical system. These factors can be provided, for example, by properly calibrating the system with an off-resonance reference particle. Our results, supported by a simple analytical model and by FDTD simulations, demonstrate the effectiveness of such experimental method in fully characterizing the optical response of a plasmonic nanoresonator.

The authors warmly acknowledge Massimiliano Labardi and Mario Agio for fruitful discussions. They also thank Witec GmBH for technical support.

*Present address: Laboratory of Physical Chemistry, ETH Zurich, 8093 Zurich, Switzerland. michele.celebrano@phys.chem.ethz.ch

[1] P. Anger *et al.*, Phys. Rev. Lett. **96**, 113002 (2006).
[2] S. Kühn *et al.*, Phys. Rev. Lett. **97**, 017402 (2006).
[3] P. Mühlschlegel *et al.*, Science **308**, 1607 (2005).
[4] P. Ghenuche *et al.*, Phys. Rev. Lett. **101**, 116805 (2008).
[5] P. Biagioni *et al.*, Phys. Rev. Lett. **102**, 256801 (2009).
[6] M. Zavelani-Rossi *et al.*, Appl. Phys. Lett. **92**, 093119 (2008).
[7] J. R. Krenn *et al.*, Phys. Rev. Lett. **82**, 2590 (1999).
[8] S. A. Maier *et al.*, Adv. Mater. **13**, 1501 (2001).
[9] E. Ozbay, Science **311**, 189 (2006).
[10] T. D. Backes and D. S. Citrin, Phys. Rev. B **78**, 153407 (2008).
[11] R. De Waele *et al.*, Nano Lett. **7**, 2004 (2007).
[12] K. L. Kelly *et al.*, J. Phys. Chem. B **107**, 668 (2003).
[13] M. Sukharev and T. Seideman, Nano Lett. **6**, 715 (2006).
[14] M. I. Stockman *et al.*, Phys. Rev. Lett. **88**, 067402 (2002).
[15] M. Aeschlimann *et al.*, Nature (London) **446**, 301 (2007).
[16] K. Lindfors *et al.*, Phys. Rev. Lett. **93**, 037401 (2004).
[17] H. J. Huang *et al.*, Opt. Express **15**, 7132 (2007).
[18] P. Stoller *et al.*, Opt. Lett. **31**, 2474 (2006).
[19] T. Klar *et al.*, Phys. Rev. Lett. **80**, 4249 (1998).
[20] A. A. Mikhailovsky *et al.*, Opt. Lett. **28**, 1686 (2003).
[21] K. Imura *et al.*, Chem. Phys. Lett. **400**, 500 (2004).
[22] M. Achermann *et al.*, Opt. Lett. **32**, 2254 (2007).
[23] C.-H. Huang *et al.*, Opt. Express **16**, 9580 (2008).
[24] C. F. Bohren and D. R. Huffman, *Absorption and Scattering of Light by Small Particles* (Wiley-VCH, New York, 1998).
[25] J. Hwang and W. E. Moerner, Opt. Commun. **280**, 487 (2007).
[26] P. Kukura *et al.*, Nano Lett. **9**, 926 (2009).
[27] J. Grand *et al.*, Phys. Rev. B **72**, 033407 (2005).
[28] L. Douillard *et al.*, Nano Lett. **8**, 935 (2008).
[29] P. Biagioni *et al.*, Appl. Phys. Lett. **87**, 223112 (2005).
[30] R. García and R. Pérez, Surf. Sci. Rep. **47**, 197 (2002).
[31] D. Gérard *et al.*, Phys. Rev. B **77**, 045413 (2008).
[32] FDTD SOLUTIONS v. 6.0.5, Lumerical Solutions Inc., Vancouver (Canada).
[33] A. A. Mikhailovsky *et al.*, Phys. Rev. B **69**, 085401 (2004).
[34] A. Drezet *et al.*, Europhys. Lett. **66**, 41 (2004).
[35] G. Wrigge *et al.*, Nat. Phys. **4**, 60 (2008).
[36] N. M. Mojarad *et al.*, J. Eur. Opt. Soc. Rapid Publ. **4**, 09014 (2009).
[37] M. Meier and A. Wokaun, Opt. Lett. **8**, 581 (1983).
[38] L. Novotny, Phys. Rev. Lett. **98**, 266802 (2007).